An Integrated Multidisciplinary Re-Evaluation of the Geothermal System at Valles Caldera, New Mexico, Using an Immersive Three-Dimensional (3D) Visualization Environment

Andrew Fowler, Scott Bennett, Maya Wildgoose, and Carolyn Cantwell

Department of Geology, University of California, Davis

Keywords

Geothermal, Valles Caldera, immersive 3D visualization, KeckCAVES, Rio Grande rift, New Mexico

ABSTRACT

We describe an approach to explore the spatial relationships of a geothermal resource by examining diverse geological, geophysical, and geochemical data sets using the *immersive* 3-dimensional (3D) visualization capabilities of the University of California – Davis (UCD) Keck Center for Active Visualization in the Earth Sciences (KeckCAVES). The KeckCAVES is a state-of-the-art facility where stereoscopic images are projected onto four, 8-foot by 10-foot surfaces (three walls and a floor). The user perceives a seamless 3D image of the data, which they can manipulate and interact with, allowing a more intuitive interpretation of data set relationships than is possible with traditional 2-dimensional (2D) techniques. Here we incorporate diverse geothermal data sets relating to the geothermal system at Valles Caldera, New Mexico including: topography, lithology, geologic structures, temperature, alteration mineralogy, and magnetotelluric information. With the ability to rapidly and intuitively observe data inter-relationships, we are able to efficiently and rapidly draw conclusions about the structure of the Valles Caldera geothermal system. The application of immersive 3D modeling to geothermal systems can provide industry with a method to make more informed assessments and cost-effective approaches for developing a key low carbon emission resource.

Introduction

Technologic advances and the drastic reduction in computational costs have resulted in the emergence of a range of software products for assembling 3D models of geospatial data (e.g. ArcScene by ESRI, 3D GeoModeller by Intrepid). Industry specific software for constructing 3D models of geospatial data has also been developed specifically for the geothermal industry (e.g. LEAPFROG software) (Cowan et al, 2002; Newson et al., 2012). The petroleum industry has utilized immersive 3D modeling for sometime (e.g. Petrel) however to the best of our knowledge *immersive* 3D technology has not yet been transferred to the geothermal industry.

Immersive 3D models differ from 2D and 3D models on a 2D computer monitor in that they allow the user to interact directly with the data. Humans perceive the world in 3D using a combination of binocular vision, motion parallax, shadow interpretation, and relative motion of objects (Harris, 2004; Billen et al., 2008). Use of a 3D immersive environment capitalizes on our ability to draw conclusions about the data that surrounds us based on our human perceptive abilities (Billen et al., 2008). In contrast, a 3D model presented on a 2D computer monitor requires constant motion to perceive depth, which compromises accurate measurement and evaluation of the displayed data (Billen et al., 2008). More traditional 2D techniques, such as maps and cross sections, limit an Earth scientist's ability to develop interpretations to few 2D planes, requiring one to extrapolate data between cross sections in their mind. Additionally, these 2D techniques typically depict a single data set. The ability to simultaneously view and interact with multidisciplinary data, spatially registered in 3D, provides a revolutionary advantage. It can reveal data interconnections that are not readily apparent when examining maps or cross-sections of differing scales and in different media. We believe that, similar to the petroleum industry, immersive 3D models of geothermal resources can be exploited to make the most informed interpretations.

The Valles Caldera contains the largest and best-studied geothermal resource in New Mexico (e.g. Hulen and Nielson, 1986; Goff et al., 1988; Shevenell et al., 1988; Sass and Morgan, 1988; Vuataz and Goff, 1989, White et al., 1992; and Goff, 2009). The goal of this assessment is not to pursue or promote development of geothermal resources in Valles Caldera, which was designated as a National Preserve in 2000, and therefore no longer accessible for commercial exploitation. Valles Caldera was chosen as an example due to the numerous publicly available geothermal-related data sets. Our approach is intended to be an example of the applicability of immersive and interactive 3D models to evaluate geothermal data sets. Modern exploration and evaluation of geo-

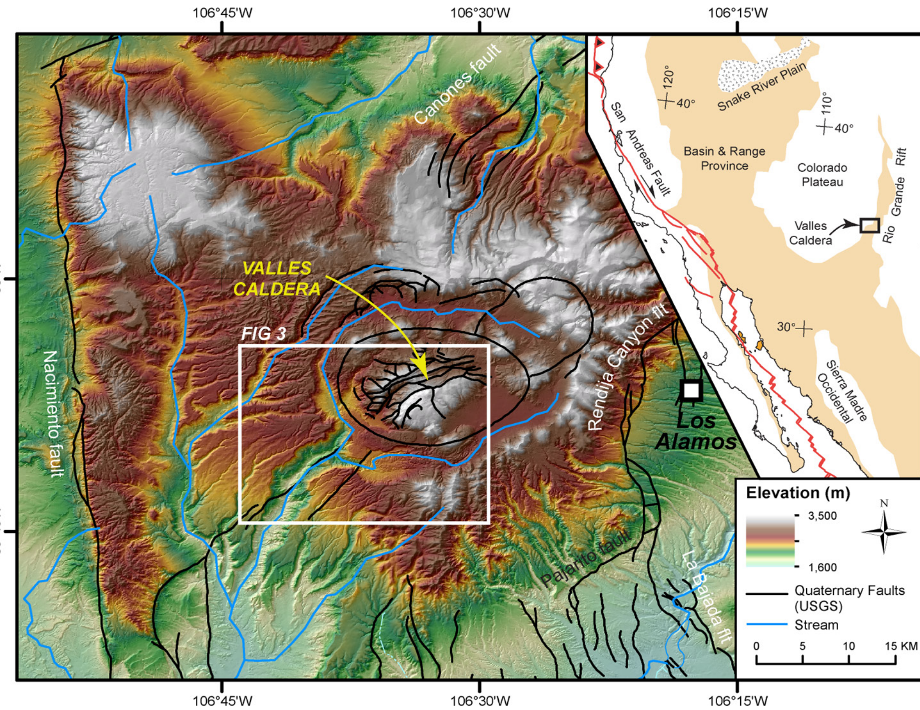

Figure 1. Location of Valles Caldera, New Mexico. Inset map shows location of Valles Caldera in context of major geologic provinces of North America.

thermal prospects routinely includes interdisciplinary teams of geologists, geochemists, and geophysicists that separately compile data and present their results using maps and cross-sections. Our approach integrates diverse data sets into a single, immersive 3D visualization model.

Geology of Valles Caldera and Region

Calderas are generally elliptical collapse features resulting from some of Earth's most powerful volcanic eruptions, and typically result in widespread volcanic ash (tuff) deposits. Calderas are often associated with hydrothermal activity (i.e. Long Valley Caldera in California and Yellowstone National Park). Valles Caldera is located in north-central New Mexico, west of the town of Los Alamos (Figure 1).

Valles Caldera lies near the southeastern edge of the Colorado Plateau and overlaps the western margin of the Rio Grande rift (Figure 1), a passive rift that has been active since ca. 36 Ma (million years before present) (Gardner et al., 1986). *Passive rifts* are believed to involve extension of the crust accompanied by passive upwelling of the hot asthenosphere, or by far-field plate tectonic pulling forces as opposed to *Active rifts,* which result from active convection of the asthenosphere. A result of the passive rifting of the Rio Grande Rift is thinned continental crust and a shallow heat source. A NE-SW trending chain of volcanic centers, the Jemez lineament, is associated with the Rio Grande rift and runs directly under Valles Caldera, and is responsible for the presence of the Jemez volcanic field (Gardner et al., 1986). Long-lived volcanism started in this area ca. 25 Ma, but the voluminous, rhyolitic eruptions responsible for the collapse and formation of Valles Caldera and deposition of the upper (Tshirege) member of the Bandelier Tuff occurred ca.1.12 Ma. Volcanism continued in the area until about 0.13 Ma (Gardner et al., 1986). The superposition of high heat flow and enhanced permeability from extensional faulting associated with the Rio Grande Rift, along with volcanic activity in the Valles Caldera are responsible for the active geothermal system.

Data Acquisition

We assembled a diversity of data sets including: geophysical, geochemical, lithological, and hydrological information for simultaneous display in the 3D environment. Integration of a wide range of variables is critical for geothermal exploration analyses, yet commonly requires the collection and interpretation of data from numerous, disparate scientific methods and sources.

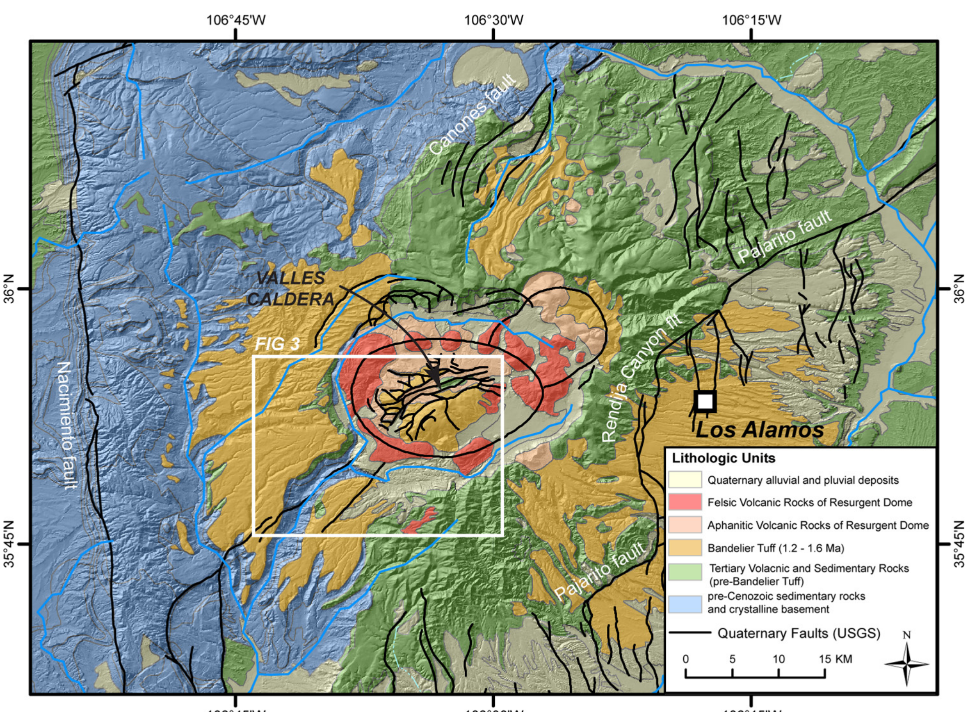

Figure 2. Geologic map of Valles Caldera region, showing key lithologic units (Green and Jones, 1997) and Quaternary faults (USGS and New Mexico Bureau of Mines and Mineral Resources, 2006). The 1.2-1.6 Ma Bandelier Tuff (orange) was deposited during the eruption that formed Valles Caldera. White box shows limits of Figure 3.

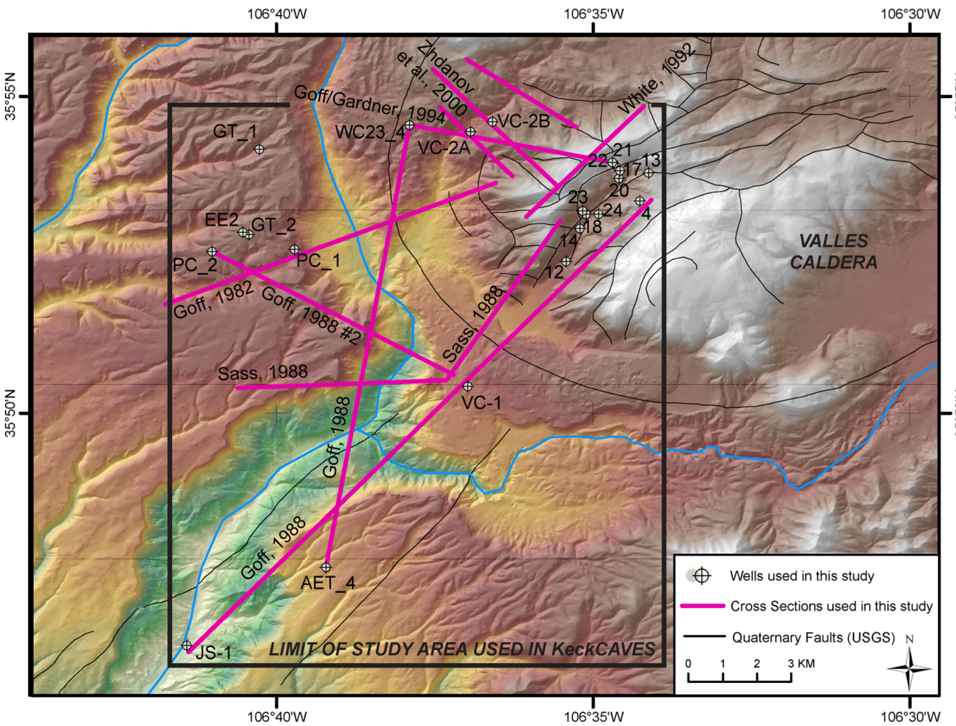

Figure 3. Map of southwestern portion of Valles Caldera, indicating the locations of wells and cross sections used in this study. Wells in the Baca geothermal field are abbreviated (e.g. Baca-12 as '12'). White box indicates limits of the 3D model produced in this study.

The majority of data utilized for this study were collected during the 1970's and 1980's, and not available in digital format. Thus, multiple methods were required to convert analog data, originally published as tables, graphs and images, into digital form.

1. **A regional geologic map** (Green and Jones, 1997) and **Quaternary fault maps** (U.S. Geological Survey and New Mexico Bureau of Mines and Mineral Resources, 2006) were acquired from the United States Geological Survey (USGS) (Figure 2). These maps highlighted the map-view extent of lithologic units and Quaternary faults that are an integral component to our geothermal analysis.

2. **Structural geology cross-sections** were compiled from Goff and Gardner (1994), Hulen and Nielson (1990), Sass and Morgan (1988), White et al. (1992), and Goff and Grigsby (1982). These cross sections depict the subsurface location of the same lithologic units and structures from the geologic map.

3. **A Digital Elevation Model (DEM)** (10-meter resolution) was acquired from the NED (National Elevation Dataset). This DEM was imported into our KeckCAVES model and provided the reference frame for all other data sets used.

4. **Borehole well data:**

A. **Temperature data** for wells used in this study were acquired from the following sources: VC-1 and EE-2 (Sass and Morgan,1988); VC-2A (Starguist,1988); VC-2B (Gardner et al., 1989); Baca-12, Baca-13, Baca-14, Baca-17, Baca-18, Baca-21, Baca-23, and Baca-24 (provided by NMBGMR, pers. comm.???); Baca-4 and Baca-20 (Hulen and Nielson, 1986); AET-4, WC 23-4, PC-1, and PC-2 (Shevenell et al.,1988); and GT-2 (Laughlin, 1977).

B. **Lithology and alteration mineralogy** data for wells used in this study were acquired from the following sources: VC-1 (Goff et al., 1986); VC-2A (Starguist, 1988); VC-2B – Gardner et al., 1989); Baca-12, Baca-20, Baca-21, Baca-22, Baca-23, and Baca-24 (Union Oil Company, 1982); AET-4, WC 23-4, PC-1, and PC-2 (Shevenell et al., 1988); GT-1, GT-2, and JS-1 (Goff et al., 1988).

Well-path deviation information for many wells was acquired from two sources (see Figure 3 for well locations): Baca-12, Baca-20, Baca-21, Baca-22, Baca-23, and Baca-24 were obtained from original well logs produced by the Union Oil Company (1982). The New Mexico Bureau of Geology and Mineral Resources (NMBGMR) provided photocopies of original drilling logs that included precise deviation data for these Union Oil wells. Estimates for the extent of deviation for wells Baca-4, Baca-13, Baca-14, Baca-17, and Baca-18 were obtained from Hulen and Nielson (1986). The remaining wells lacked deviation information and were assumed to be vertical.

5. **Three magnetotelluric (MT) profiles** were obtained from Zhdanov et al. (2000). These three profiles are sampled slices that were selected by Zhdanov et al. (2000) as representative profiles from their 3D magnetotelluric survey. Although gridded 3D magnetotelluric data could be easily incorporated into the model, only the cross-sectional data were publically available.

6. A **regional gravity map** of the Valles Caldera was digitized from Wilt and Vonder Haar (1986).

Data Preparation Methodology

To present geospatial data in 3D, latitude (X), longitude (Y), and elevation (Z) values need to be assigned to data set elements. Here we discuss how we digitally assigned X, Y, Z values to multiple analog data sets analyzed in our Valles Caldera geothermal model.

Borehole Well Data

Borehole logs of temperature and alteration mineralogy were first digitized from analog, paper records. A critical step in the data preparation methodology was correcting digitized data for well deviation from vertical.

Temperature

Temperature data were digitized using a MatLab script (imagepick3) developed by Professor James McClain at UC Davis specifically for this project. Images of temperature logs were converted to JPEG format and imported into MatLab. Once the depth and temperature axes were specified, selecting points along the temperature-depth curve at dense intervals with a mouse resulted in digitized temperature-depth data. Temperature values were then assigned to the corrected X-Y-Z value of the corresponding well.

Alteration Mineralogy

The first appearance of key alteration minerals in a geothermal well is an important indicator of subsurface temperature (e.g. Tómasson and Kristmannsdóttir, 1972). The first downhole occurrence of alteration minerals were determined and tabulated for pyrite, chlorite, and epidote for each of the wells listed below:

Pyrite: Baca 4, Baca-12, Baca-17, VC-2A, Baca-20, Baca-21, Baca-22, Baca-23, and Baca-24.

Chlorite: Baca 4, Baca-12, Baca-17, VC-2A, VC-2B, Baca-20, Baca-21, and Baca-24.

Epidote: Baca 4, Baca-12, Baca-17, Baca-20, Baca-21, Baca-22, Baca-23, and Baca-24.

Well Deviation Correction

Well deviation is the lateral shift from vertical as a well is drilled. To plot well deviation in 3D, each point down a well must have an X, Y, and Z coordinate. However, the depth values recorded on deviated well logs were *downhole* depths. *Downhole depth* is equivalent to the length of the drilling rods boring out the well. If a well is deviated from vertical, the *downhole depth* can vary significantly from the *true vertical depth* below the ground surface, and the discrepancy increases as the well depth increases. Additionally, the location of the well in the subsurface becomes further from the wellhead location. If well deviation is not taken into account, significant error can result in datasets (i.e. temperature and alteration mineralogy) referenced to uncorrected downhole depths.

Wells with deviation data fell into 3 categories:

1. Wells with precise deviation data: Baca-12, Baca-20, Baca-21, Baca-22, Baca-23, and Baca-24.

2. Wells with estimated deviation from well surface trace maps: Baca-13, Baca-14, Baca-17, Baca-18, and Baca-24.

3. Wells with no deviation data: VC-1, VC-2A, VC-2B, AET-4, WC 23-4, PC-1, PC-2, GT1, GT-2, and JS-1.

Category 1 well deviations were precisely calculated using a combination of trigonometry and GIS software (Result shown on Figure 4).

Category 2 well deviations were calculated by importing a well surface trace map from Hulen and Nielson (1986) into ArcGIS, georeferencing the map, and reading X and Y (latitude and longitude) coordinates directly. The depths associated with each point along the well surface trace were estimated. This was achieved by partitioning the well surface trace into portions of equal length between the known top-of-well and bottom-of well elevations. While this method is not entirely accurate, it provided better estimates for true depth and X-Y coordinates of subsurface well data than treating the wells as vertical.

Category 3 wells were not corrected for deviation due to lack of available deviation data and were assumed to be vertical.

3D Temperature Grid

In order to create 3D temperature data set for our KeckCAVES model, multiple horizontal temperature slices were produced from extrapolation of the corrected downhole temperature data. Eleven horizontal temperature slices were created, spaced vertically at

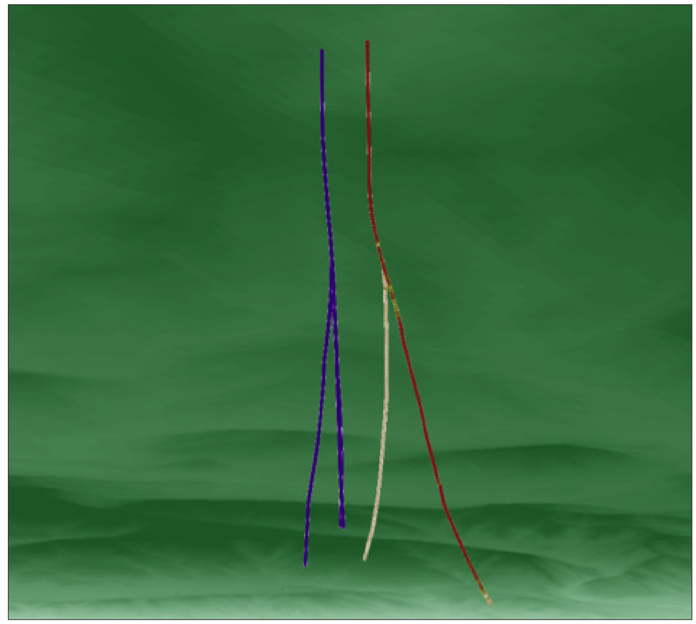

Figure 4. Oblique subsurface example of final product of well deviation calculation for the Baca-20 and Baca-22 wells (shown in ArcScene). View is looking up from beneath topography.

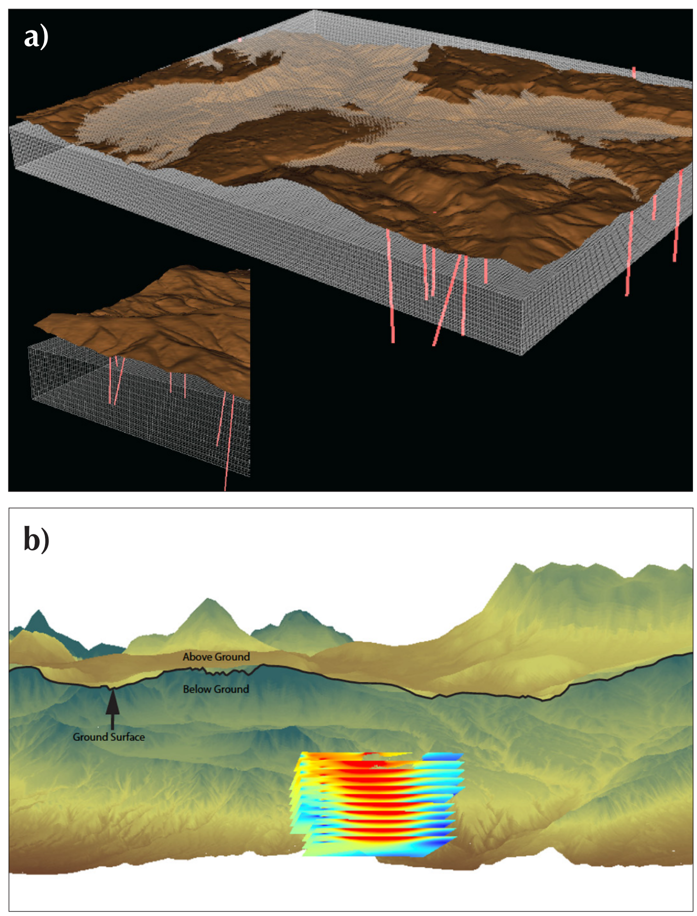

Figure 5. (a) Example of 3D temperature grid generated in KeckCAVES (left) and (b) interpolated temperature slices at 100m intervals using ArcGIS (bottom): view is looking obliquely up from beneath topography; topography edge is seen in this view as a sharp transition from tan to blue.

100 m intervals, between 1500 and 2500 meters asl (above sea level) (Figure 5, right side) using the ArcGIS Inverse Distance Weighted (IDW) tool. Temperature values from these surfaces were then converted to a continuous 3D grid of cells with 50 m by 50 m (horizontal) and 100 m (vertical) dimensions and visualized as a 3D data volume in the KeckCAVES (Figure 6, left side).

Alteration Mineralogy Isosurfaces

The tabulated alteration mineralogy files were imported into ArcGIS and a raster surface was interpolated for each mineral using the IDW tool. The raster pixel values were equivalent to the elevation of the first occurrence of each respective mineral. Not all wells were adequately logged with respect to alteration mineralogy. Wells inadequately logged were ignored and the corresponding raster surfaces were extrapolated through these wells. The three raster surfaces (pyrite, chlorite, and epidote) were then exported for display in our KeckCAVES model (Figure 6).

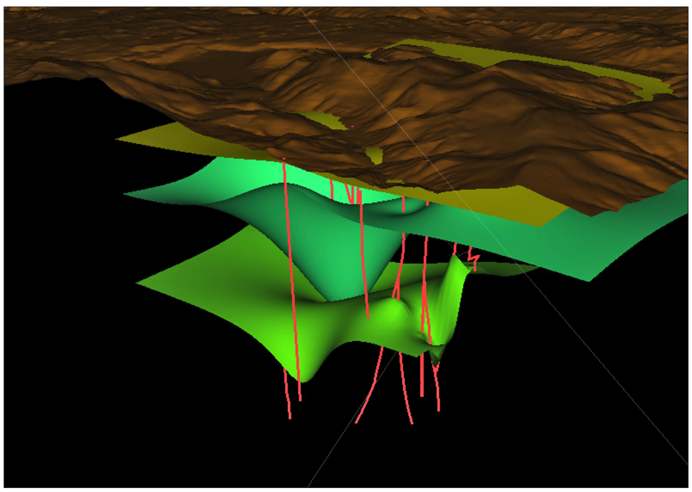

Figure 6. View of interpolated surfaces of alteration mineralogy in KeckCAVES; olive green (upper) = pyrite, dark green (middle) = chlorite, pistachio green (lower) = epidote.

Cross Sections

Lithologic, structural, and geophysical cross-sections from various sources were incorporated into the 3D model. Lithologic units were simplified and shaded for continuity across various authors. The 3D coordinates (X, Y, and Z) were determined for the four corners of each cross-section. Cross-section lines were digitized as vertical planes. Cross-sections with bends were treated as adjacent, but distinct cross sections, oriented at different azimuths. Using the known X-Y-Z location of each corner of the cross sections, a raster image of each section was 'hung' in 3D space, below the DEM in our KeckCaves model.

The KeckCAVES Facility

The KeckCAVES facility is a three-sided room with a three walls and a floor, each measuring 8 X 10 feet. Stereoscopic images are projected onto each surface. A tracking system synchronizes the projected stereo images with the position and orientation of a user's head, producing a seamless 3-dimensional environment within which both the user and the data exist and can interact. The stereopairs of images alternate rapidly, and the user wears head-tracked goggles that oscillate alternating polarity synchronously with the rapidly flickering stereo images, generating a smooth, natural 3D view. The user interacts with the data using a 5-button tracked wand, which allows smooth maneuvering of the data and the implementation of a suite of interactivity tools (Figure 7).

The Virtual Reality User Interface (VRUI) that runs the KeckCAVES was developed by Dr. Oliver Kreylos of the UCD Institute for Data Analysis and Visualization (IDAV) and supports data manipulation programs used to interactively render 3D volumes (3DVisualizer), display illuminated terrain (TerrainViewer), and mount static georeferenced elements such as bore holes, vertical cross-sections, and maps. The functionality of these two programs (3DVisualizer and TerrainViewer) was combined for this project to generate a viewer for Valles Caldera data that encompasses an interpolated temperature volume, terrain from a DEM, 3D well paths, alteration mineralogy surfaces, and a collection of structural, lithological, and geophysical cross-sections (Figure 8). Each element among this collection of data could be displayed independently or in conjunction with other data elements, and accurately geolocated within our 3D model of the southwestern portion of the Valles Caldera.

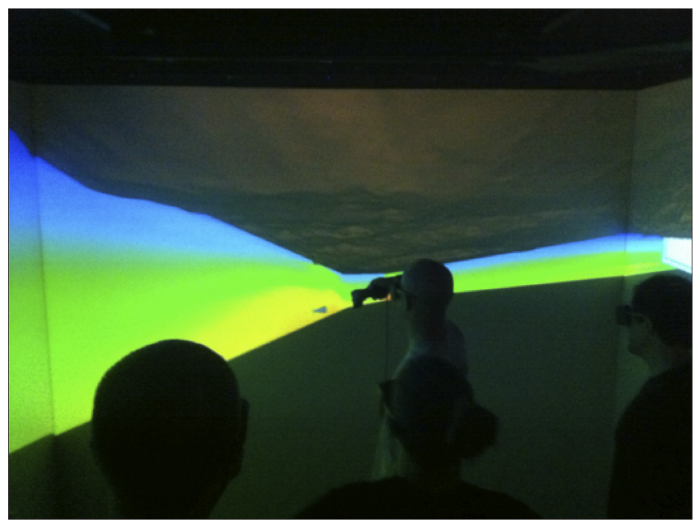

Figure 7. Students Andrew Fowler, Maya Wildgoose and Austin Elliott in the KeckCAVES facility, viewing temperature isosurfaces.

Interactive tools in the KeckCAVES allowed us to dynamically display and inspect temperature isosurfaces (isotherms) in order to infer zones of hydrothermal upwelling and areas dominated by cold meteoric water recharge. We were able to assign a completely customizable color ramp to the temperature range, and the KeckCAVES program allowed us to reach into the data volume and drag the wand around, generating a dynamic isotherm at the temperature represented by whichever grid cell the cursor occupies. We also generated and made observations of static isotherms of 100°C, 150°C, 200°C, and 250°C (Figure 8), which were useful while integrating other data sets (e.g. lithologic cross sections, surface traces of Quaternary faults, or magnetotelluric profiles).

The temperature field can also be visualized as any number of arbitrarily-oriented slices (Figure 9), or published cross-sections from our literature search (Figure 10). Again, the color ramp used

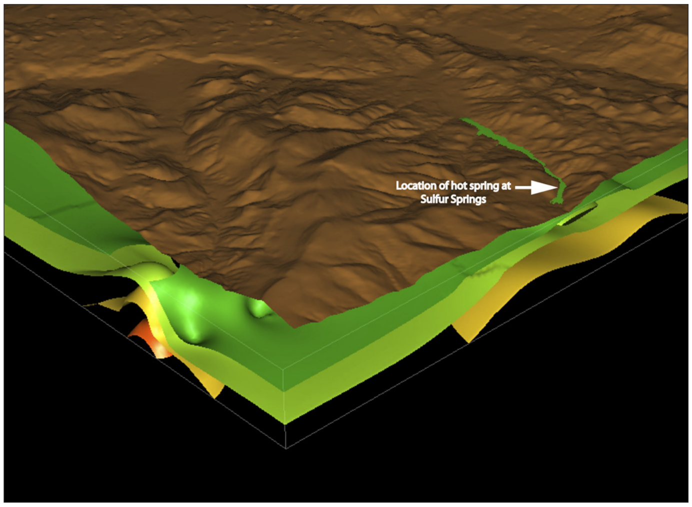

Figure 8. (100°, 150°, 200° and 250° C) Static temperature isotherms displayed in KeckCaves. View shows the NE corner of study area looking SW. The 100° C isotherm (darkest green) intersects the ground surface coincident with the surficial hot springs in the Sulfur Springs area.

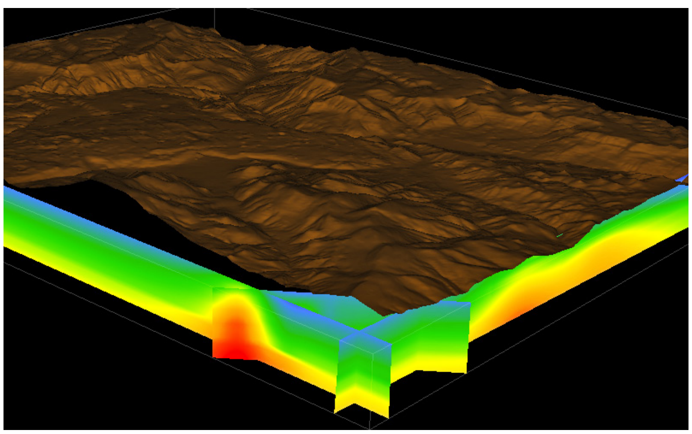

Figure 9. Arbitrarily-oriented temperature slices can be selected by the user. View is from NE corner of study area looking SW.

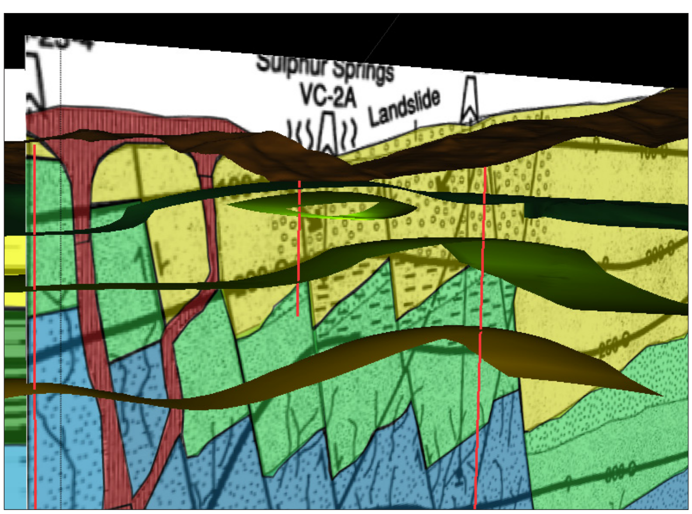

Figure 10. Example of static visualization element (cross sections) displayed in conjunction with temperature surfaces.

to display the temperature range is completely customizable, and a particular palette can be saved and reloaded for display of additional visualization elements (i.e., slices or isosurfaces).

In a more graphically compelling mode, the full temperature volume can be rendered as a color-scaled semi-transparent "haze" (Figure 11). This visualization mode highlights structures within the volume.

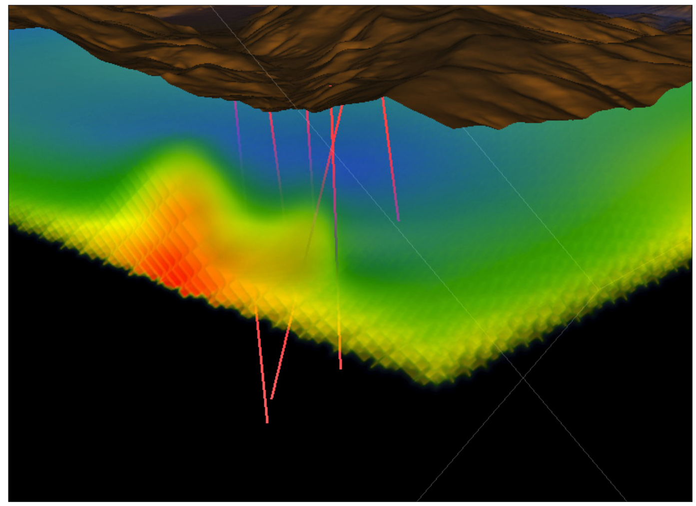

Figure 11. Volume filling temperature "haze".

Results

The integration and evaluation of multiple datasets in immersive 3D space revealed the following relationships for Valles Caldera.

Temperature Relationship to Hot Springs

The 100°C isotherm intersects the ground surface in the topographically low Sulfur Springs area. The intersection of these data sets is coincident with the location of known surface hot springs.

Temperature Relationship to Faults and Topography

Integration of surface topography with calculated temperature data revealed both high and low temperature anomalies. We identified a pronounced low-temperature anomaly in the Baca well field (Figure 12). Additionally, we identified two high temperature anomalies, one in the Baca well field and one in the Sulfur Springs area.

The low temperature anomaly in the Baca well field is coincident with a NE-SW trending fault co-located in a NE-SW trending drainage that cuts across the resurgent dome within the caldera ring fracture. We interpret this low-temperature anomaly as recharge zone, where the topographic drainage likely focuses cold surface waters into the subsurface along the fault plane (Figure 13). The ground surface elevation above this low-temperature anomaly in the resurgent dome ranges from approximately 2700 to 2900m. This elevation is consistent with the hydrothermal recharge elevation of 2530 to 2890m proposed based on oxygen and hydrogen isotope studies by Vuataz and Goff (1986). Vuataz and Goff (1986) suggest that recharge occurs within the caldera depression between the elevations of the caldera walls and the peak of the resurgent dome. They speculate that recharge occurs in broad moat valleys in the north and east of the caldera: Valle San Antonio, Valle Toledo, and Valle Grande. Our model suggests that recharge is occurring to some extent along faults and fractures within the resurgent dome. However, it should be noted that our model is of limited aerial extent, and this recharge zone likely extends beyond our model limits, possibly towards, Valle Toledo.

The Baca well field high temperature anomaly is adjacent to and west of the Baca low temperature anomaly (Figure 12). The Baca high-temperature anomaly is likely associated with fluid upflow along adjacent and parallel faults and fractures.

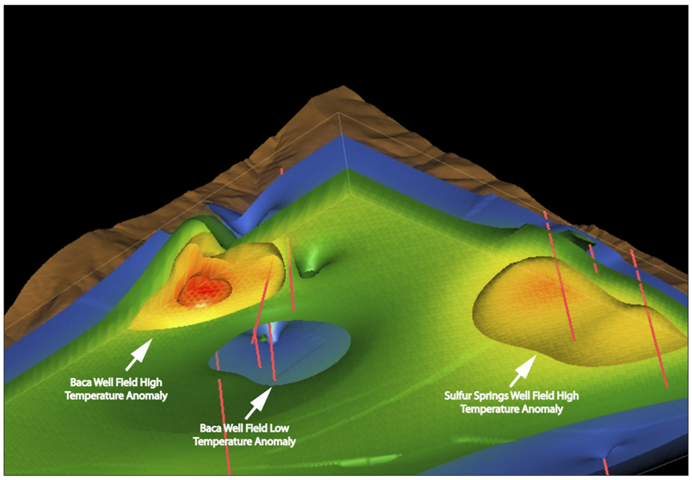

Figure 12. A low temperature anomaly is expressed as "hole" or discontinuity in the green 150° C temperature surface. The Baca well field and heat anomaly are to the left and the Sulfur Springs heat anomaly is to the right. The NE corner of the model is visible in this view. The intersection of the 100° C isotherm (blue) with the bottom of the model (on the lower right) correlates strongly with the location of the caldera ring fracture.

The Sulfur Springs high-temperature anomaly corresponds to a concentration of normal faults observed on cross sections integrated into our model (Figure 10). These normal faults are likely conduits for upward flow of heated fluids within the caldera ring fracture. The cross sections also reveal that temperatures exceeding 200°C coincide within the lower portion of Paleozoic units and the upper part of the crystalline basement, which both underlie the Bandelier Tuff.

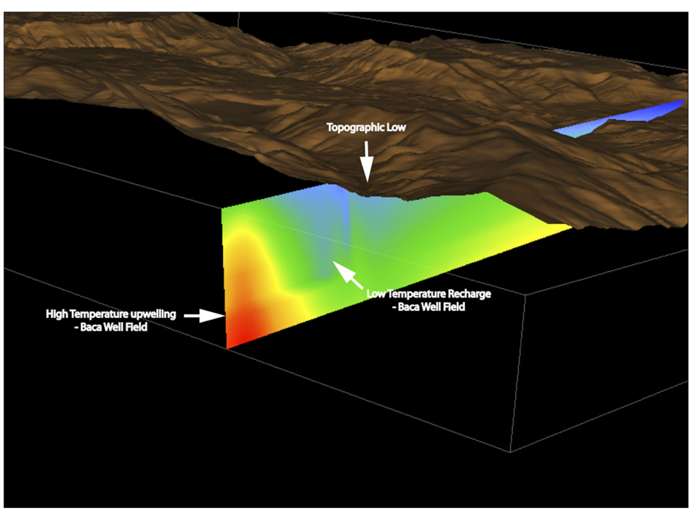

Figure 13. Correlation between a fault controlled topographic low and a low temperature anomaly in the Baca well field. The red-colored high temperature anomaly (convex upward) is associated with the Baca geothermal field.

Recharge along the caldera ring fracture appears to be a barrier to heat transfer out of the caldera. One exception to this is the hydrothermal outflow zone to the southwest, which follows the Jemez Fault Zone and San Diego Valley. Our model indicates that temperature isotherms gradually taper off outside of the ring fracture (Figure 12). This suggests that rocks beyond the ring fracture are relatively impermeable and we speculate that this helps to protect and isolate the Valles Caldera hydrothermal system from far-field cold water recharge.

Overall, high temperature geothermal resources appear to occur on the flanks of NE-SW fractures in the resurgent dome, near the Baca well field. Similarly oriented fractures also appear to control cooler meteoric recharge. High temperature resources likely extend eastwards beyond the boundary of our model.

Temperature Relationship to Apparent Resistivity and Stratigraphy

Our model suggests a correlation between apparent resistivity from Zhdanov et al. (2000) and our extrapolated temperature volume (Figure 14). Low apparent resistivity in the Zhdanov magnetotelluric profiles coincides with higher temperature isosurfaces displayed in our model. Broadly, temperatures in our model exceeding 150°C correlate with approximately 3 to 10Ωm resistivity. Temperatures in our model exceeding 200°C correlate with approximately <3Ωm resistivity.

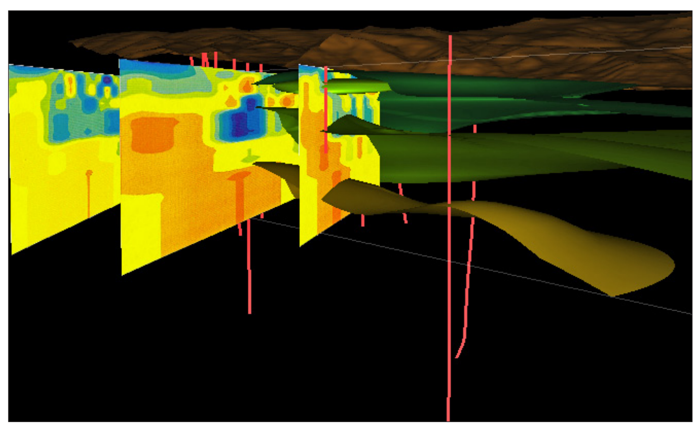

Figure 14. Static apparent resistivity measurements from Zhdanov et al. 2000 shown with temperature isosurfaces.

Temperature Comparison With Previous Models

There is general agreement between previous temperature models and the one presented in this study. Small discrepancies exist between previous temperature estimates (shown on integrated cross-sections) and our calculated temperature volume. One possible explanation for these discrepancies is that temperatures are often projected onto cross-sections from nearby wells and cannot take into account the 3D variability of temperature. Another explanation for variability in different temperature models is that other models may be using temperature data from a different well gauging event. We have attempted to incorporate the most recent (equilibrated) temperature logs available, but have unlikely used an identical dataset as previous models.

Alteration Mineralogy

The first occurrence of pyrite (Figure 15) is approximately 50 to 100m below ground surface, and does not correlate with temperatures. Pyrite occurrence does not appear to relate to our model temperatures. A likely explanation for the shallow occurrence of pyrite is precipitation due to increase in the pH in the shallow geothermal system due to degassing of CO_2, or boiling.

The first occurrence of chlorite is consistent with a model temperature of approximately 120°C (Figure 15). The chlorite isotherm during metamorphism can occur as low as 100°C in low temperature environments (DeCaritat et al., 1993). Our results indicate that chlorite formation is a modern phenomenon in the geothermal system.

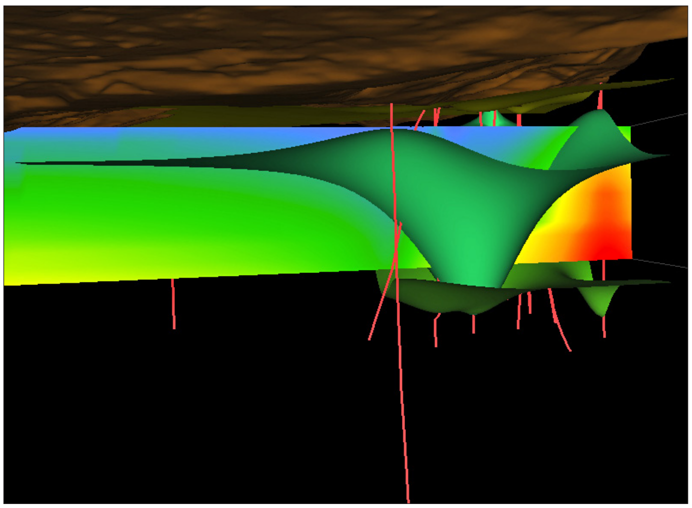

Figure 15. The first occurrence of chlorite (darker green surface) correlates well with the subsurface temperature dataset.

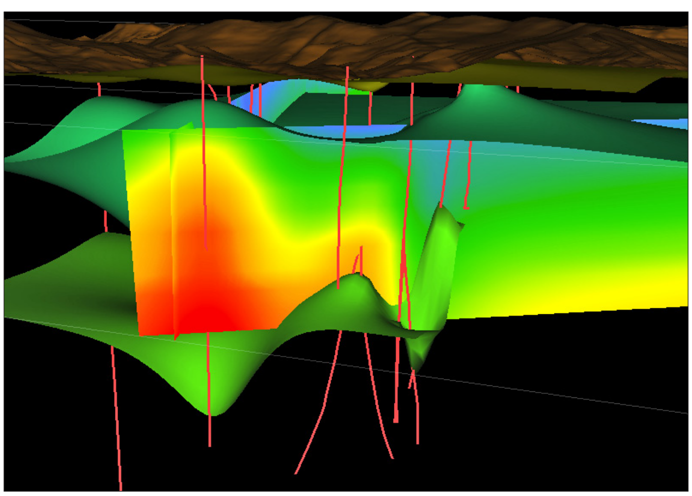

Figure 16. The first occurrence of epidote (lowest, "pistachio" green) surface correlates poorly with temperature (red-green-blue vertical slice). Above the epidote surface is the chlorite (darker green) and pyrite (olive green) surfaces. The chlorite surface correlates well with temperature in this view, similar to Figure 15.

Epidote generally occurs in hydrothermal systems at temperatures of 200°C to 350°C (Arnason and Bird, 1992). The first occurrence of epidote (Figure 16) matches model temperatures of approximately 220°C. This relationship indicates that epidote formation is related to modern geothermal temperatures. However, the first occurrence of epidote in some wells is associated with lower temperatures of approximately 120°C and in other wells at temperatures in excess of 250°C (Figure 16). One explanation is that epidote is recording a previous phase in hydrothermal circulation. Another explanation is that epidote was misidentified in the well logs. The discrepancy between the epidote data sets incorporated into our model highlights an area that requires further evaluation.

Project Applications

Geological, geophysical, and hydrological relationships that were not obvious when considering individual data sets became readily apparent when multiple data sets were integrated and displayed in an immersive 3D environment. An essential aspect of a geothermal resource assessment is an estimation of the extent and volume of the resource. To this end, our model is a powerful tool to:

1. Facilitate volume estimates of the area contained below a given isotherm. Identifying stratigraphic units that are likely to host geothermal resources can be done using 2D cross-section data; however, our 3D stratigraphic model leads to easy quantification of resources. For example, in our model, the intersection of the volume below the 250°C isotherm and the Precambrian basement, which has significant fracture permeability, provides an improved volume estimate of the geothermal resource.

2. Constrain boundaries of a fracture dominated geothermal resource by displaying the relationship between the 3D temperature field and surface faults. Our 3D model also facilitates subsurface projection of faults. Although we did not have access to seismic data, projection of microearthquakes can identify the fault planes at depth and can highlight areas of fractured rock that may indicate potential locations of increased permeability and active hydrothermal flow.

3. Integrate quantitative resistivity models with subsurface stratigraphy, alteration, temperature, and structural data—an approach that few studies have attempted. Integrating these data sets provides a better understanding of the origin of resistivity trends so that anomalies associated with hydrothermal alteration or flow of conductive geothermal fluids can be more readily distinguished from anomalies related to lithologic/stratigraphic variations.

4. Compare temperature isotherms to isothermal surfaces inferred from alteration minerals. This juxtaposition provides insight into the long-term temperature evolution of a geothermal system based on alteration mineralogy. For example, the presence of high temperature alteration min-

erals at depths shallower than the inferred temperature of formation suggests local cooling of the geothermal system. The relative shapes of the 3D temperature surfaces could indicate if the entire system is in decline or if the focus of hydrothermal upflow is migrating with time.

Our unique approach could be enhanced and made more powerful by integrating additional data sets, such as: loss of circulation data, fracture zones in well logs, heat flow data, microseismicity data, seismic profiles, groundwater contours, and chemical and isotopic data. A major benefit of our model is that it can be rapidly and iteratively updated as new data is acquired.

The current iteration of our model has revealed the following insights into the geothermal system at Valles Caldera:

- The initial onset of chlorite is closely associated with the 120ºC isotherm. The first occurrence of hydrothermal minerals identified in drill cuttings may be useful temperature proxies.
- Resistivity values below 3Ωm generally correlate with temperatures above 200ºC. Low resistivity relates to elevated temperatures and may be used to locate geothermal resources.
- High and low temperature anomalies correlate strongly with fault locations. This relationship demonstrates the importance of fracture controlled fluid flow in the Rio Grande Rift.
- Geothermal fluid recharge occurs at faults within the resurgent dome in addition to along the ring fractures. This relationship indicates that fluid recharge for hydrothermal systems can be very localized.

Conclusions

No single technique or measurement can be used to evaluate geothermal resources. These resources are complicated, mutually unique, interactive systems that inherently require multidisciplinary tactics before we can begin to understand their controls. Technologic advance and the drastic reduction in computational cost now allow us to readily incorporate a diverse array of digital data sets into 3D models that enhance our understanding of the systems and facilitate our efforts to quantitatively assess resources.

We have developed an integrated multidisciplinary re-evaluation of the geothermal system at Valles Caldera, New Mexico. Valles Caldera is a national preserve and exempt from geothermal development, which we are not advocating in this area. This re-evaluation of Valles Caldera examines data sets from previous studies within an immersive, 3D environment at the UCD KeckCAVES. We have utilized the KeckCAVES facility to explore, manipulate, and create an immersive, interactive 3D model of the Valles Caldera geothermal system as an example of an approach for improved geothermal assessment.

Acknowledgments

We would like to thank the following people, including both faculty and students at UC Davis for their help finding, organizing, and processing the large amount of data that we used in this project: Dr. Peter Schiffman, Dr. Robert Zierenberg, Dr. James McClain, Dr. William Glassley, Lesley Barnes, Samuel Hawkes, Rita Martin, and Rachael Johnson.

We also gratefully acknowledge the help and guidance of the KeckCAVES facility group, including Louise Kellogg and Austin Elliott. In particular, we'd like to thank Oliver Kreylos for his effort in writing a program to help us integrate 2D and 3D data in the CAVES.

References

Arnason, John G. and Bird, Dennis K, 1992, Formation of Zoned Epidote in Hydrothermal Systems: Water-Rock Interaction-proceedings of the 7th international symposium on water-rock interaction, 13-18th July, 1992.

Ankeny, L. A., and Braile, L. W., 1986, Upper Crustal Structure Beneath the Jemez Mountains Volcanic Field, New Mexico, Determined by Three-Dimensional Simultaneous Inversion of Seismic Refraction and Earthquake Data: Journal of Geophysical Research, v. 91, no. B6, p. 6188-6198.

Billen, M. I., Kreylos, O., Hamann, B., Jadamec, M. A., Kellogg, L. H., Staadt, O., and Sumner, D. Y., 2008, A geoscience perspective on immersive 3D gridded data visualization: Computers & Geosciences, v. 34, no. 9, p. 1056-1072.

Bodvarsson, G. S., Vonder Haar, S., Wilt, M., and Tsang, C. F., 1982, Preliminary Studies of the Reservoir Capacity and the Generating Potential of the Baca Geothermal Field, New Mexico: Water Resources Research, v. 18, no. 6, p. 1713-1723.

Cowan, E. J., Beatson, R. K., Fright, W. R., McLennan, T. J., and Mitchell, T. J., 2002, Rapid geological modelling: Applied Structural Geology for Mineral Exploration and Mining, International Symposium (Kalgoorlie, 23-25 Spetember 2002).

DeCaritat, P., Hutcheon, I., and Walshe, J. L., 1993, Chlorite Geothermometry - A Review: Clays and Clay Minerals, v. 41, no. 2, p. 219-239.

Gardner, J. N., Goff, F., Garcia, S., and Hagan, R. C., 1986, Stratigraphic relations and lithologic variations in the Jemez volcanic field, New Mexico: Journal of Geophysical Research, v. 91, no. B2, p. 1763-1778.

Gardner, J. N., Goff, F., Goff, S., Maassen, L., Mathews, K., Wachs, D., and Wilson, D., 1987, Core lithology, Valles caldera No. 1, New Mexico: Los Alamos National Lab., NM (USA), LA-10957-OBES; Other: ON: DE87010831.

Gardner, J. N., Hulen, J. B., Lysne, P., Jacobson, R., Goff, F., Nielson, D. L., Pisto, L., and Criswell, C. W., 1989, Scientific core hole Valles Caldera 2b (VC-2b), New Mexico - drilling and some initial results: Los Alamos National Lab., NM (USA), LA-UR-89-2025; CONF-891031--2.

Goff, F., 2009, Valles Caldera, University of New Mexico Press.

Goff, F., and Gardner, J. N., 1994, Evolution of a mineralized Geothermal System: Economic Geology, v. 89, p. 1803-1832.

Goff, F., Gardner, J. N., Hawkins, W., and Goff, S., 1986, Initial Results from VC-1, first continental scientific drilling program core hole in Valles Caldera, New Mexico: Journal of Geophysical Research, v. 91, no. B2, p. 1742-1752.

Goff, F., Shevenell, L., Gardner, J. N., Vuataz, F. D., and Grigsby, C. O., 1988, The Hydrothermal Outflow Plume of Valles Caldera, New Mexico, and a Comparison With Other Outflow Plumes: Journal of Geophysical Research, v. 93, no. B6, p. 6041-6058.

Green, G.N., and Jones, G.E., 1997, The Digital Geologic Map of New Mexico in ARC/INFO Format: U.S. Geological Survey Open-File Report 97-0052, 9 p.; http://pubs.usgs.gov/of/1992/ofr-92-0052.

Harris, J. M., 2004, Binocular vision- moving closer to reality: Transactions of the Royal Society of London, Annum 362, p. 2721-2739.

Hulen, J. B., and Nielson, D. L., 1986, Hydrothermal Alteration in the Baca Geothermal System Redondo Dome, Valles Caldera, New Mexico: Journal of Geophysical Research, v. 91, no. B2, p. 1867-1886.

Hulen, J. B., and Nielson, D. L., 1990, Possible Volcanotectonic Controls on High-temperature Thermal Fluid up flow in the Valles Caldera, New Mexico: Geothermal Resources Council Transactions, v. 14, Part II p. 1457-1464.

Newson, J., Mannington, W., Sepulveda, F., Lane, R., Pascoe, R., CLearwater, E., and O'Sullivan, M. J., 2012, Application of 3D modelling and visualization software to reservoir simulation: LEAPFROG Geothermal and TOUGH2: Proceedings of the Thirty-Seventh Workshop on Geothermal Reservoir Engineering. Stanford University, California, January 30 - February 1, 2012.

Tómasson, J. and Kristmannsdóttir, H., 1972 High temperature alteration minerals and thermal brines, Reykjanes, Iceland. Contributions to Mineralogy and Petrology, v. 36, p. 123-134.

Laughlin, A. W., Pettitt, R. A., West, F. G., Eddy, A. C., Balagna, J. P., and Charles, R. W., 1977, Status of the Los Alamos experiment to extract geothermal energy from hot dry rock: Geology, v. 5, no. 4, p. 237.

Sass, J. H., and Morgan, P., 1988, Conductive Heat Flux in VC-1 and the Thermal Regime of Valles Caldera, Jemez Mountains, New Mexico: Journal of Geophysical Research, v. 93, no. B6, p. 6027-6039.

Segar, R., 1971. Quantitative gravity interpretation Valles Caldera area, Sandoval and Rio Arriba Counties, New Mexico. Union Oil Internal Report.

Shevenell, L., Goff, F., Miles, D., Waibel, A., and Swanberg, C., 1988, Lithologic Descriptions and Temperature Profiles of Five Wells in the Southwestern Valles Caldera Region, New Mexico, LA-11165-OBES; Other: ON: DE88007158.

Starguist, V. L., 1988, Core log: Valles caldera No. 2A, New Mexico: Los Alamos National Lab., NM (USA), LA-11176-OBES; Other: ON: DE88007156.

Union Oil Company, 1982, Final report, Baca project, geothermal demonstration power plant, report prepared for U.S. Department of Energy, 436 pp., San Francisco Operations Office, San Francisco, California.

U.S. Geological Survey and New Mexico Bureau of Mines and Mineral Resources, 2006, Quaternary fault and fold database for the United States, accessed DATE, from USGS web site: http//earthquakes.usgs.gov/regional/qfaults/.

Vuataz, F. D., and Goff, F., 1986, Isotope Geochemistry of Thermal and Non-thermal Waters in the Valles Caldera, Jemez Mountains, Northern New Mexico.: Journal of Geophysical Research, v. 91, no. B2, p. 1835-1853.

White, A.F., Chuma, N.J. and Goff, F., 1992. Mass transfer constraints on the chemical evolution of an active hydrothermal system, Valles caldera, New Mexico: Journal of Volcanology, v. 49, p. 233-253.

Zhdanov, M. S., Fang, S., and Hursan, G., 2000, Electromagnetic inversion using quasi-linear approximation: Geophysics, v. 65, no. 5, p. 1501-1513.